Available online at www.sciencedirect.com
SCIENCE DIRECT®
Journal of Catalysis 224 (2004) 94–106
JOURNAL OF CATALYSIS
www.elsevier.com/locate/jcat

Hydrodesulfurization reaction pathways on MoS_2 nanoclusters revealed by scanning tunneling microscopy

J.V. Lauritsen,[a,*] M. Nyberg,[b] J.K. Nørskov,[b] B.S. Clausen,[c] H. Topsøe,[c] E. Lægsgaard,[a] and F. Besenbacher[a]

[a] *Center for Atomic-scale Materials Physics, Interdisciplinary Nanoscience Center (iNANO), and Department of Physics and Astronomy, University of Aarhus, DK-8000 Aarhus C, Denmark*

[b] *Center for Atomic-scale Materials Physics and Department of Physics, Technical University of Denmark, Lyngby, Denmark*

[c] *Haldor Topsøe A/S, Nymøllevej 55, DK-2800 Lyngby, Denmark*

Received 11 December 2003; revised 3 February 2004; accepted 9 February 2004

Abstract

Single-layer MoS_2 nanoclusters were synthesized on a Au substrate as a model system for the hydrotreating catalyst and studied by atomically resolved scanning tunneling microscopy (STM) in order to achieve atomic-scale insight into the interactions with hydrogen and thiophene (C_4H_4S). Surprisingly, STM images show that thiophene molecules can adsorb and react on the fully sulfided edges of triangular single-layer MoS_2 nanoclusters. We associate this unusual behavior with the presence of special brim sites exhibiting a metallic character. The STM images reveal that these sites exist only at the regions immediately adjacent to the edges of the MoS_2 nanoclusters, and from density-functional theory such sites are found to be associated with one-dimensional electronic edge states. The fully sulfur-saturated sites are from STM images found to be capable of adsorbing thiophene, and when thiophene and hydrogen reactants are coadsorbed here, a reaction path is revealed which leads to partial hydrogenation of the thiophene followed by C–S bond activation and ring opening of thiophene molecules. This may be regarded as important first steps in the hydrodesulfurization of thiophene. The metallic brim sites are suggested to be important for other hydrotreating reactions over MoS_2-based catalysts, and the properties of the brim sites directly explain why hydrogenation reactions of aromatics are not severely inhibited by H_2S. The presence of brim sites in MoS_2 nanoclusters also explains previous structure–activity relations and observations regarding steric effects and the influence of stacking of MoS_2 on the reactivity and selectivity.

Keywords: Hydrodesulfurization; Hydrotreating; Model catalyst; Scanning tunneling microscopy; Density-functional theory; Thiophene; MoS_2; Active sites; Edge states; Nanoclusters; Steric effects; Poisoning

1. Introduction

Hydrotreating processes are reductive hydrogen treatments of fossil fuel applied to upgrade and clean up oil resources to reduce the emission of environmentally harmful compounds and to sustain a better exploitation of low-grade crude oil. In view of the new demands for ultralow sulfur transport fuels, special attention is being directed toward the catalytic hydrodesulfurization (HDS) process [1–5]. Alumina-supported molybdenum disulfide (MoS_2) or tungsten disulfide-based (WS_2) hydrodesulfurization catalysts have for many years been the most important catalysts for this service [6,7], and the active phase in the catalyst is now generally accepted to be present as few nanometer wide, single-layer, MoS_2-like nanoparticles, usually promoted with Co or Ni. Despite numerous studies of this catalyst, it has, however, not been possible to resolve a number of fundamental issues related to the catalyst structure and reactivity with the traditional tools for catalyst characterization. To improve the hydrotreating catalyst and to reach the new tight fuel specifications a more detailed and fundamental understanding of how the catalyst operates in needed.

Based on studies of structure–reactivity relationships, the HDS activity has been attributed to sites located at the edges of MoS_2 nanoclusters (see e.g., [6] and references therein). Furthermore, it has commonly been suggested that active sites in the form of sulfur vacancies or so-called coordinatively unsaturated sites (CUS) are created in a reaction with hydrogen which strips off one or more sulfur atoms from

* Corresponding author.
E-mail address: jvang@phys.au.dk (J.V. Lauritsen).

0021-9517/$ – see front matter
doi:10.1016/j.jcat.2004.02.009

the MoS_2 nanocluster edges. It is proposed that these low-coordinated point defects will have a high affinity for bond formations with the hetero-atom in sulfur-bearing oil molecules, thereby facilitating the sulfur extraction, but little direct evidence for the existence of vacancies under typical reaction conditions has been presented, nor has their role in the catalytic cycle been clarified. A further complication is that HDS of thiophene-based molecules is believed to proceed by different pathways—the so-called direct and hydrogenation routes [2,5,6], and kinetic and poisoning studies indicate that the involved catalytic sites may be different. Again, these sites have been suggested to be associated with edge vacancies but with different degrees of coordinatively unsaturation [8]. Several spectroscopic studies have indicated that S–H groups may form [6,9,10], and some of these studies have indicated that such groups may also be located at the edges of the MoS_2 clusters [11]. Consequently, the S–H groups have been proposed to play an important role in the formation of both vacancies and in hydrogenation reactions of unsaturated compounds in the oil feed, but again only little direct insight exists on the role of S–H groups for the different reactions. A better description of the active cluster edges and their interaction with the reactants seems to be a prerequisite for a deeper understanding of the catalyst activity and selectivity.

Atom-resolved scanning tunneling microscopy studies (STM) studies of catalyst model systems have recently given the first direct insight into the atomic-scale structure of MoS_2 nanoclusters and the promoted CoMoS structures [12–14]. The model systems consisted of a few nanometer wide, gold-supported MoS_2 and CoMoS nanoclusters, and with the STM it was possible to characterize their geometrical and electronic structure in great detail. On this basis, new important insight was obtained on the nanocluster morphology, on the atomic-scale structure of the catalytically important edges, and on the formation of sulfur vacancies. It was also shown that the nanocluster morphology and exact edge structures were sensitive to reaction conditions [14]. Recently, we have taken such studies one important step further and used the STM on HDS model catalysts to study the adsorption and reaction of thiophene (C_4H_4S) with atomic resolution. A brief report of some of the results was given in [15] and presently we will discuss these results in greater detail. Our choice of model system for the HDS catalyst enables us for the first time to pinpoint with atomic resolution the sites on the MoS_2 nanoclusters where thiophene interacts, and to resolve signatures of reaction intermediates from the reaction. We observe an unusual chemical activity associated with the regions adjacent to the edges of MoS_2 nanoclusters, which we show to be able to hydrogenate and break up thiophene molecules (C_4H_4S) in the presence of hydrogen. Remarkably, this reaction is found to proceed on the fully sulfided MoS_2 nanoclusters, which are normally regarded as chemically inactive. This surprising type of chemistry therefore does not involve interaction with sulfur vacancies. Rather, it is shown to be associated with the presence of one-dimensional electronic edge states, which give the regions adjacent to the edges of the MoS_2 nanoclusters a distinct metallic character. We explain the observed reaction pattern with the fact that the metallic edges (the so-called brim sites), unlike the insulating and inactive basal plane of MoS_2, have the ability to donate and accept electrons just like ordinary catalytically active metals. The reaction leads to the formation of adsorbed thiolate (R–S) intermediates which are much more reactive and therefore readily desulfurized, and the observed reaction pattern may then be considered as a first step in the hydrodesulfurization of thiophene. It is furthermore seen that many controversial results reported in the literature may now be explained by considering reactions involving the brim sites, and we propose that the type of adsorption and hydrogenation on the metallic brim sites may be important for the hydrogenation of aromatic compounds in general.

2. Methods

2.1. Scanning tunneling microscopy

The experiments are performed in a standard ultra-high vacuum (UHV) chamber with a base pressure below 1×10^{-10} mbar. The system is equipped with standard surface science equipment and the high-resolution, variable-temperature Aarhus STM [16,17], capable of providing atom-resolved images on a routine basis at temperatures down to 140 K.

In the industrial-type HDS catalysts, the active nanoclusters are typically supported on γ-Al_2O_3, but this kind of substrate is electrically insulating and is therefore not suitable for STM studies. Instead we use the Au(111) surface as a model substrate for the synthesis of MoS_2 nanoclusters. The rather inert nature of gold means that we can study the intrinsic properties of the MoS_2 nanoclusters. Furthermore, this surface exhibits the so-called herringbone reconstruction, which provides an ideal template of nucleation sites for deposited metal atoms and thereby supports the dispersion of submonolayer amounts of Mo into nanoclusters. In Fig. 1a the Mo deposited on the gold is seen to be regularly distributed into nanoclusters located in the elbow regions of the Au(111) herringbone reconstruction. For the synthesis of MoS_2 nanoclusters, we have developed a scheme where we first deposit Mo at a coverage of $\approx 10\%$ of a monolayer in an H_2S gas environment corresponding to 1×10^{-6} mbar, and subsequently anneal the sample to 673 K while keeping the sulfiding atmosphere. This procedure results in a highly dispersed ensemble of 20–30 Å wide single-layer MoS_2 nanoclusters. An example of an STM image of the HDS model system used for the present studies is given in Fig. 1b. Further details of the synthesis and characteristics of the MoS_2 nanoclusters are presented in Refs. [12,14].

Liquid-phase thiophene (99% Aldrich) is contained at room temperature in a glass test tube which is pumped sep-

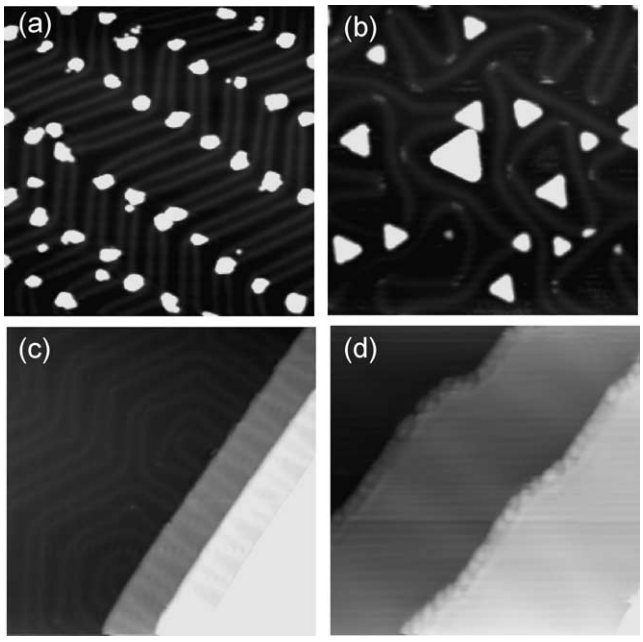

Fig. 1. (a) STM image (572 × 590 Å^2) showing the Mo nanoclusters formed on the Au(111) surface by physical vapor deposition of metallic Mo. (b) STM image (404 × 409 Å^2) of single-layer MoS_2 nanoclusters synthesized on the Au(111) surface as a model system for the hydrotreating catalyst. (c) STM image (572 × 590 Å^2) of the clean Au(111) surface and step edges after exposure to thiophene vapor at room temperature. No bonding is observed. (d) STM image of the Au(111) surface after exposure to thiophene at temperatures below 180 K. Thiophene molecules are observed to adsorb near the step edges but not on the Au(111) terraces.

arately, and the thiophene vapor is admitted to the UHV chamber by means of an all-metal leak valve and a doser tube. Prior to every experiment, the thiophene is purified by freeze–pump–thaw cycles. Experiments are conducted at sample temperatures in the range 180 K up to 500 K. Cooling is achieved by placing the sample in the STM, which allows the sample to reach temperatures of approximately 140 K. Line-of-sight between the thiophene doser and the sample placed in the compact STM is, however, not possible, and during thiophene dosage the sample is picked up by a manipulator and moved to the thiophene doser. For the experiments with a cooled sample, the relevant temperature is therefore the maximum temperature achieved during this operation before the sample is repositioned in the cold STM. Similarly, for the high-temperature experiments the experimental conditions refer to the lowest sample temperature registered during thiophene dosage. After the high-temperature dosages of thiophene, the sample was quickly quenched to room temperature and imaged with the STM.

To test the affinity of the Au(111) model substrate, thiophene was initially dosed onto the clean Au(111) surface. As seen in the STM image in Fig. 1c, no bonding of thiophene could be observed on the terraces of the Au(111) at room temperature by the exposures applied in this study. This is in agreement with previous theoretical investigations [18] and a recent XPS study [19]. Additionally, this serves as a purity check of the thiophene vapor against contamination of, e.g., thiols, which bind fairly strongly to the Au surface [20–22]. Only by exposing the surface to thiophene at sample temperatures below 180 K did STM images (Fig. 1d) reveal signatures of thiophene molecules adsorbed at the step edges of the Au(111) surface. Even at these low temperatures thiophene molecules could, however, not be observed on the terraces, demonstrating the inertness of the model substrate.

2.2. Density-functional theory

The theoretical calculations are based on density-functional theory (DFT) performed within the generalized gradient approximation using ultrasoft pseudopotentials to describe the ion cores [23–25]. The edges of the MoS_2 nanoclusters are modeled by a stripe of MoS_2. When repeated in a supercell geometry, the MoS_2 stripe is terminated by infinitely long $(10\bar{1}0)$ Mo edges and $(\bar{1}010)$ S edges, respectively [26]. For simulations of STM spectra we used a rather large unit cell which is six Mo layers wide across (y) and two Mo broad along the stripe (x). The structures and energies were calculated for a smaller unit cell which was 4 Mo wide, and either 2 or 3 Mo broad. All structures are completely relaxed and transition states are located by constrained relaxation, taking care that the reaction pathways become continuous as in the nudged elastic band method [27]. The Kohn–Sham orbitals were expanded in plane waves with a cutoff energy of 25 Ry, and 8 special k points in the k_x direction. Simulated STM images of the MoS_2 edges are calculated on the basis of the Tersoff–Hamann formalism [28] where the tunneling matrix elements are evaluated using the self-consistent KS wave functions.

3. Results

The starting point for the experiments reported in this paper is a catalyst model system consisting of highly dispersed 2- to 3-nm-wide, gold-supported, single-layer MoS_2 nanoclusters similar to those studied previously [12,14]. These studies have shown that the MoS_2 nanoclusters deviate considerably in geometry and electronic structure from what is commonly assumed from the bulk properties of MoS_2. In the following we will show that such effects, which dominate entirely for the smallest MoS_2 clusters, are very important for the reactivity, and in order to understand the new results it is necessary to highlight some of the structural and electronic features of the MoS_2 nanoclusters in some detail (see also Refs. [12,14,29]).

3.1. One-dimensional metallic edge states in MoS_2 nanoclusters

Fig. 2 shows an atomically resolved STM image of a single-layer MoS_2 nanocluster. Like the cluster in this figure, the vast majority of the MoS_2 nanoclusters formed by the synthesis procedure described above are found in STM

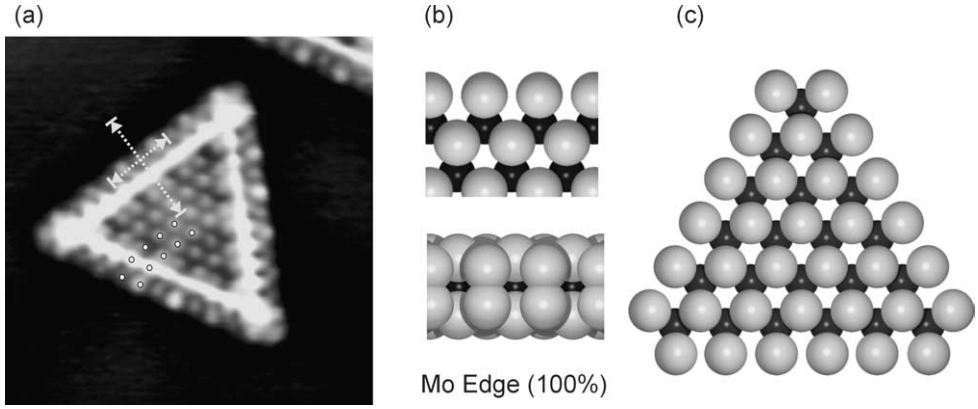

Fig. 2. (a) Atom-resolved STM image ($V_t = -6.1$ mV, $I_t = 1.29$ nA) of a triangular single-layer MoS_2 nanocluster (67×69 Å^2). White dots superimposed near the edge of the cluster indicate the registry of edge protrusions. Lines in the image refer to the line scans marked with triangles in Fig. 3. (b) Ball models in top and side view of the edge structure, the Mo edge with S dimers (S, bright; Mo, dark). (c) Ball model of a MoS_2 triangle exposing this type of edge termination.

images (Fig. 1b) to adopt a triangular shape, reflecting that this is indeed the equilibrium shape under the present sulfiding conditions. The observed triangular shape immediately implies that the single-layer MoS_2 nanoclusters are terminated by only one of two low-indexed edge terminations, the $(10\bar{1}0)$ Mo edges or the $(\bar{1}010)$ S edges; see Refs. [26, 30–33]. The question of which type of edge that actually terminates the triangular cluster is complicated by the fact that each of the edges may have a varying amount of S adsorbates and exist in several different configurations. By means of STM we can determine directly the type of edges which terminate the triangular MoS_2 nanoclusters formed under the sulfiding conditions used in this study. Other synthesis conditions have been shown to result in different types of edge structures [14,34], but here we exclusively deal with the structures formed under the most sulfiding conditions.

In the atom-resolved STM image displayed in Fig. 2a, the triangular MoS_2 nanocluster is seen to display a flat basal plane with protrusions arranged in a hexagonal pattern and an interatomic distance of 3.15 ± 0.1 Å. This is in perfect agreement with the interatomic distances of the S atoms on the (0001) basal plane structure of bulk MoS_2. From atom-resolved STM images, the edge protrusions are furthermore found to be imaged *out of registry* with the basal plane S atoms. In fact, the protrusions are shifted half a lattice constant along the edge, but retain the bulk interatomic distance of ~ 3.15 Å. Intuitively, a simple way of interpreting the edge structure would be to assign it to a reconstructed Mo edge where the S atoms on the edge have shifted half a lattice constant and moved down into the plane of the Mo atoms. Geometrically this configuration seems to be consistent with the observed shift of half a lattice constant in the STM image. Such a purely geometrical interpretation of the STM images is, however, not generally valid since the images reflect a rather complicated convolution of the geometric and the electronic structure of the surface, and not only geometrical information. In this respect, the electronic structure of the MoS_2 cluster is very interesting, since bulk MoS_2, consisting of infinite sheets of S–Mo–S, is semiconducting with a bandgap of ≈ 1.2 eV [35,36]. According to the Tersoff–Hamann theory [28], low-bias STM images in the constant-current mode reflect, to a first-order approximation, contours of constant local density of electronic states (LDOS) at the Fermi level of the surface structure projected onto the position of the tip apex. The absence of electronic states at the Fermi level available for tunneling in bulk MoS_2 thus implies that the clusters should be impossible to image at bias voltages numerically lower than half the value of the bandgap. This is clearly not the case, as shown in Fig. 2a, and it is found experimentally that STM images of the MoS_2 clusters are possible at low tunneling bias. In particular, a pronounced bright brim of high electron state density is seen in the STM image in Fig. 2a to extend all the way around the cluster edge adjacent to the edge protrusions. A line scan across the cluster edge shows that the bright brim is imaged approximately ~ 0.4 Å higher than the basal plane. A line scan parallel to and directly on top of the bright brim reveals no systematic corrugations in this direction. Rather than a geometrical effect, the brim is associated with an electronic effect probed by the STM, reflecting subtle changes at the edges. The appearance of the bright brim on the nanoclusters thus suggests that electrons are localized strongly into one dimension perpendicular to the MoS_2 edges, but delocalized along the direction of the edges.

A detailed theoretical calculation of the electronic structure reveals that the MoS_2 nanoclusters have so-called *one-dimensional edge states* with a distinct metallic character, and that these are responsible for the unusual features observed with STM [26,29]. In these studies, density-functional theory calculations have been performed on both unsupported and gold-supported MoS_2 slabs exposing the Mo edge and S edge, and in terms of STM simulations they have helped identify the exact structure of the edges. The triangular MoS_2 nanoclusters (Fig. 2) were determined to be terminated by Mo edges fully saturated with S dimers. This configuration is depicted in Fig. 2b, and the model shows

that the sulfur atoms at the edge laterally coincide with the bulk S lattice, but they display a small pairing perpendicular to the MoS_2(0001) surface thus forming S_2 dimers or disulfide-like species [30,31]. Importantly, the calculations furthermore reveal that the electronic band structure for this particular type of edge has *two* electronic edge states which cross the Fermi level and therefore render the MoS_2 edges metallic and conductive, as observed with STM. A detailed analysis reveals that one of the metallic edge states is almost completely localized at the S dimers. It is a superposition of p_x orbitals extending in two parallel chains along the edge. This edge state has a maximum in between the S atoms and a node at the geometrical position of the S atoms. Interestingly, the protrusions in the STM images on the edge are therefore not associated with the position of the S dimers, but rather reflect the electronic structure in the interstitial region between pairs of S dimers. The other metallic edge state is somewhat more complicated and is primarily constituted by two bonds: (i) the *d–d* bond between the first row of Mo atoms, and (ii) the *p–d* bond between the second row of S atoms and the Mo atom behind. When this is included in the STM simulation, the theoretical model of the Mo edge with S dimers is seen to fully reproduce the STM findings, and the bright brim observed in the row adjacent to the edge protrusions is therefore associated with the second metallic edge state. Hence, we concluded that MoS_2 nanoclusters are terminated by Mo edges which are fully sulfur covered. From a coordination-chemistry point of view, such saturated structures are normally not considered to be particularly reactive. As we shall see in the next sections, however, the metallic edges give the MoS_2 nanoclusters a completely different chemistry than what has ordinarily been assumed.

3.2. Thiophene adsorption on MoS_2 nanoclusters

First we have investigated the interaction of thiophene with the freshly prepared single-layer triangular MoS_2 nanoclusters. The HDS model system is exposed to thiophene at room temperature and studied with STM. The room temperature experiments do not reveal any interaction on the (0001) basal plane of the MoS_2 nanoclusters, in accordance with previous TPD studies of thiophene on single crystal MoS_2(0001) [37]. Additionally, the STM images of the MoS_2 nanoclusters show that the edges, which are fully sulfided, appear to be unaffected with respect to adsorption of thiophene at room temperature.

Even when the temperature of the sample is lowered below 200 K, we do not see any interaction of thiophene on the (0001) basal plane of the MoS_2 nanoclusters. At these temperatures, however, individual thiophene molecules are observed in the STM images to be adsorbed near the edges of the MoS_2 nanoclusters. The thiophene molecules, which are imaged as large protrusions with a dimension matching the expected van der Waals radius of thiophene ($\sim 4 \times 5$ Å), are in fact observed in two different adsorption modes, as depicted in Fig. 3a: (A) on the Au substrate decorating the cluster periphery, and (B) on top of the edges of the MoS_2 nanoclusters.

A rough estimate of the adsorption strength for the two different adsorption modes of thiophene can be found in terms of their apparent desorption temperature by heating the sample slightly in the manipulator, followed by imaging of the sample in the still cooled STM. This is illustrated by the sequence of STM images, Figs. 3a–c, obtained of MoS_2 clusters at different substrate temperatures. The thiophene molecules decorating the periphery of the nanocluster (type A) are seen to desorb at temperatures around 240 ± 10 K, indicating that thiophene is weakly bonded in this adsorption configuration. From the rather low corrugation of less than 0.4 Å above the Au(111) in the STM image, the thiophene appears to be adsorbed in a flat geometry on the Au(111) substrate. Possibly, this adsorption mode of thiophene is a result of dipole–dipole interactions with the cluster edge, combined with some sort of interaction between the π-system of thiophene and the Au substrate. Most likely, this binding of thiophene is of a noncovalent character and can be characterized as a physisorbed state of little relevance to the catalytic properties of the cluster. The weak bonding is further underlined by an apparent large distance of ~ 4 Å from the molecule to the peripheral edge atoms of the MoS_2 nanoclusters.

On the other hand, the thiophene species adsorbed on top of the edges of the MoS_2 nanoclusters (type B) can be attributed to a direct interaction between thiophene and the clusters. Here, thiophene is, however, also weakly bound and is not imaged at temperatures exceeding 200 ± 10 K. Interestingly, the sites where thiophene molecules adsorb here are associated with the bright brim; i.e., it appears to involve a direct interaction with sites on the metallic edge state of the Mo edge. In contrast to the common assumption that the fully saturated edges generally do not bind thiophene, the results clearly suggest that the special electronic environment present here may facilitate the formation of stable chemical bonds. Again, a rather low corrugation and the position and dimension of the protrusions associated with the molecules suggests that the nature of the bonding is associated with π-bonding at sites on top of the edge state. In the terminology of organometallic chemistry this corresponds to a flat η^5 adsorption geometry, which in this case does not refer to a coordination to a single metal atom but rather to the delocalized metallic edge state. Thiophene adsorbed in an η^5 configuration was also previously found to be predominant at low temperature in several vibrational spectroscopic studies on supported MoS_2/alumina samples [38–40]. Since heating the sample slightly above 200 K results in desorption of the molecules for the on-top site, it is concluded that this configuration is also a relatively weakly adsorbed state. In the present context it should be noted, however, that thiophene binds considerably stronger to the metallic edge state than to internal regions of the MoS_2 basal plane. The low-temperature results thus provide information on a possible

initial adsorption geometry of thiophene on the edges, which under the right conditions may lead to further reactions.

3.3. Thiophene on H-activated MoS_2 nanoclusters

In view of the results for the adsorption of thiophene above, it is highly interesting that *only* when the triangular MoS_2 nanoclusters are pretreated with atomic hydrogen, a much stronger chemisorbed state is observed in atom-resolved STM images (see Fig. 4). The experiments are performed using a "quench-and-look approach," where the model system is first heated to 673 K and exposed to atomic hydrogen produced by dissociating H_2 on a glowing W filament. The H flux is then terminated and the clusters are ex-

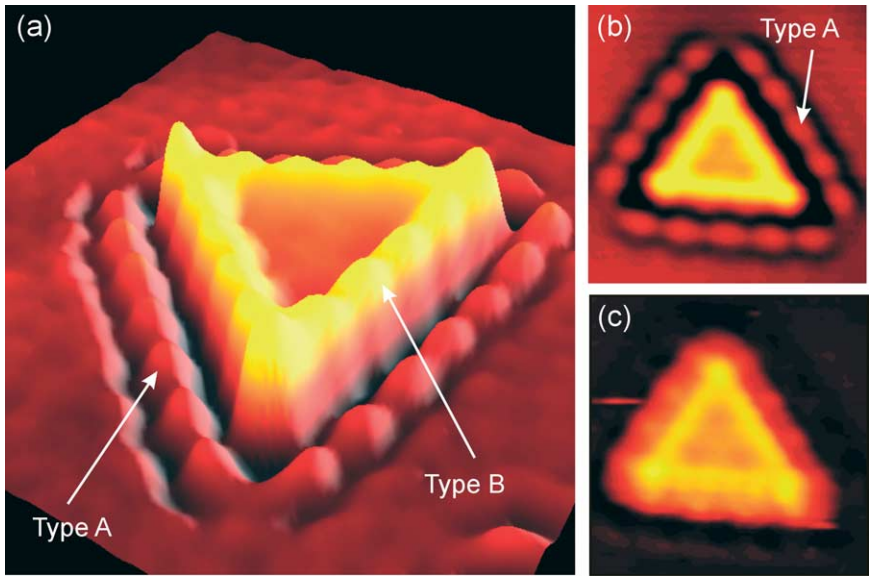

Fig. 3. Three STM images of a triangular single-layer MoS_2 nanocluster illustrating the bonding of thiophene at low temperatures. The images are listed in the order of increasing substrate temperature (T). (a) When T is below 200 K thiophene adsorbs molecularly in two different configurations. The 3D rendering of the STM image shows thiophene molecules adsorbed in positions on top of the bright brim associated with an edge state (type B), and additionally thiophene decorates the perimeter of the cluster (type A). (b) STM image representative for the temperatures in the interval 200 K $< T <$ 240 K, where thiophene molecules on top of the brim have desorbed, whereas the perimeter decoration is retained. (c) At temperatures $T >$ 240 K no indication of adsorbed thiophene was observed with STM.

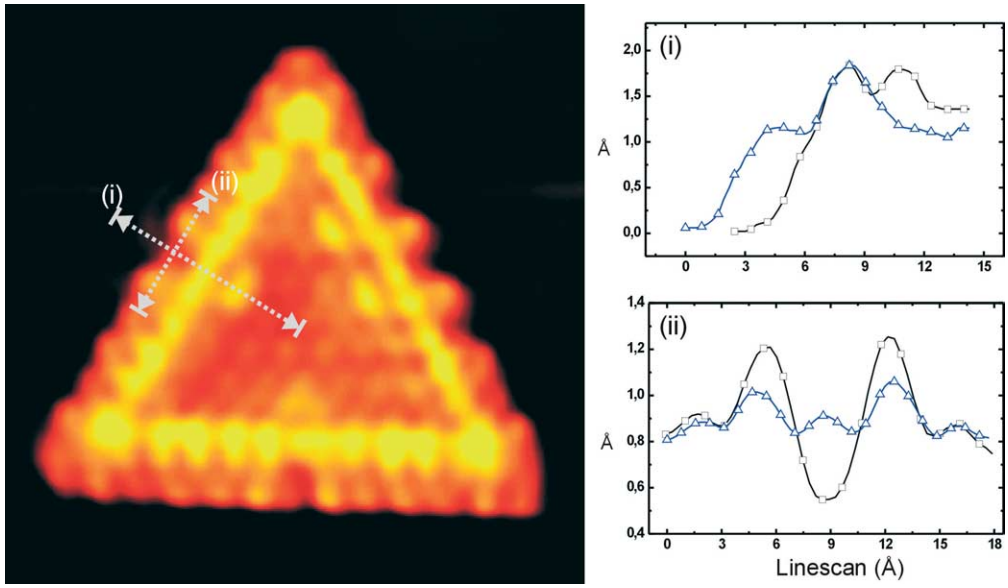

Fig. 4. Atom-resolved STM image ($V_t = -331$ mV, $I_t = 0.50$ nA) of an atomic hydrogen pretreated MoS_2 cluster, which was subsequently exposed to thiophene. Image dimensions are 50×54 Å^2. The individual molecules adsorbed on sites associated with the metallic edge state are identified by the bean-like features adjacent to the bright brim (see line scan (i)) and the shifted intensity of the outermost edge protrusions relative to the clean edge (triangles refers to the clean edge). These shifts in intensity are shown in line scan (ii) and are associated with changes in the local electronic structure as observed with STM upon molecule adsorption.

posed to thiophene at an elevated sample temperature around 500 K. Subsequently the model system was quenched to room temperature and imaged with the STM.

The atomically resolved STM image in Fig. 4 shows one of the triangular single-layer MoS_2 nanoclusters following the exposure to first atomic hydrogen and subsequently thiophene. Several "bean-like" structures are observed to protrude ~ 0.4 Å from the basal plane in the row adjacent to the bright brim of the MoS_2 cluster. This is also illustrated in Fig. 4, where two STM line scans performed on the edges before and after reaction with thiophene and hydrogen are compared. These bean-like features can be associated with individual molecules bonded to sites on the metallic edge state. From line scan (ii) performed along the edge of the MoS_2 nanocluster in Fig. 4, it is furthermore concluded that the adsorption of each molecule is always accompanied by a decrease in intensity (~ 0.4 Å) of the edge protrusions located in front of the bean-like structure, and a slight increase (~ 0.2 Å) at the two neighboring protrusions relative to the Mo edge of the clean MoS_2 nanocluster. Additionally, a detailed inspection of the close-up in Fig. 7a reveals that the bean-like features are slightly asymmetric with respect to the corresponding edge depression.

As already pointed out in Section 3.1, STM images generally reflect a rather complex convolution of the electronic and geometric structure, and combined with the highly perturbed electronic structure which already dominates the edges of the triangular MoS_2 clusters, relating the observed new structures in Fig. 4 to the molecular structure of reaction products or intermediates from a HDS reaction is a difficult task. Most likely, the shifted intensity of the protrusions near the adsorption site is the result of a slight quenching of the metallic edge state that is associated with the S dimers. Such a phenomenon is observed in the close vicinity of adsorbates on substrates with spatially confined states in general, for example, surface states which are the two-dimensional analogues to edge states [41,42]. The bean-like features can, on the other hand, be ascribed directly to a part of the structure of the adsorbed molecules, which are placed in a position astride the bright brim associated with a metallic edge state.

Several observations show that the molecules observed with STM cannot in any conceivable way reflect intact thiophene molecules coordinated end-on to either one or more S vacancy sites (i.e., undercoordinated Mo atoms on the cluster edge). First of all, the cluster edges in Fig. 4 display all the characteristics of the fully sulfided Mo edge, i.e., the pronounced 0.4 Å high bright brim and the edge protrusions which are all shifted exactly half a lattice constant out of registry. Mo edges which are partially or completely reduced with respect to sulfur coverage do exist under different conditions, but they are imaged with a quite different structure in STM images [14]. Secondly, we find that the adsorbed molecules are quite mobile; i.e., they can jump from one site to the next, as imaged in the consecutive series of STM images in Fig. 9. At no instance were vacancies found to exhibit the same mobility in STM images at room temperature. We therefore conclude that the adsorbed species are coordinated to the fully sulfided Mo edges, and that the molecules must be intermediates from a chemical reaction occurring on the metallic brim sites. Since these reaction intermediates are only observed when the clusters have been preexposed to atomic hydrogen, the chemical properties of the MoS_2 clusters must have changed substantially upon exposure with atomic H. We therefore propose that S–H groups are formed during the H exposure and that these play an essential role in a reaction with thiophene occurring on sites on the metallic brim.

3.4. Hydrogen activation

We have investigated the interaction of both molecular and atomic hydrogen with the MoS_2 nanoclusters in some detail with STM and find that most types of reactions with molecular hydrogen (H_2) are inhibited under the conditions of the experiments. We associate this with a rather high activation barrier for dissociation of H_2 and the low pressures used in the experiment. Reactions with predissociated (atomic) hydrogen, however, change the appearance of the cluster edges in STM images significantly. We have previously shown that the use of atomic hydrogen in the experiments can produce small amounts of sulfur vacancies on the edges of the clusters [12], but in addition to this, a detailed analysis of the STM images shows that also the appearance of edges with no decreased sulfur content changes. After exposure to atomic hydrogen, little qualitative change is seen on the edges which still have the characteristics of the fully sulfided Mo edges; i.e., protrusions are still out of registry and the 0.4 Å high bright brim seems unaltered. A detailed analysis of a large number of atom-resolved STM images reveal, however, that the fully sulfided edges in the clusters display a small intensity shift of the outermost edge protrusions after exposure to atomic hydrogen. This is best illustrated with STM line scans, as shown in Fig. 5a, where data for the edge on the freshly prepared fully sulfided structures are compared with a similar line scan for an atomic hydrogen pretreated cluster. The average height of the edge protrusions is seen to shift down relative to the basal plane by ~ 0.2 Å for the H-treated cluster. This downshift occurs upon atomic hydrogen treatments, and therefore suggests that the observations are related to the formation of S–H groups on the fully sulfided edges. We interpret the intensity reduction in the STM images as a modification of the LDOS at the Fermi level in the interstitial regions between S dimers when H species saturate the edges. This is supported by recent DFT-based theoretical studies of different hydrogen configurations of H on MoS_2 edges [26]. In these studies, accordance with the STM results is found for a configuration in which H adsorbs on the S dimer in a position immediately adjacent to the bright brim, see Fig. 5b. The STM simulation of this configuration in Fig. 5c shows only a slight qualitative change of the edges upon H adsorption; i.e., the high intensity of the brim is retained and edge pro-

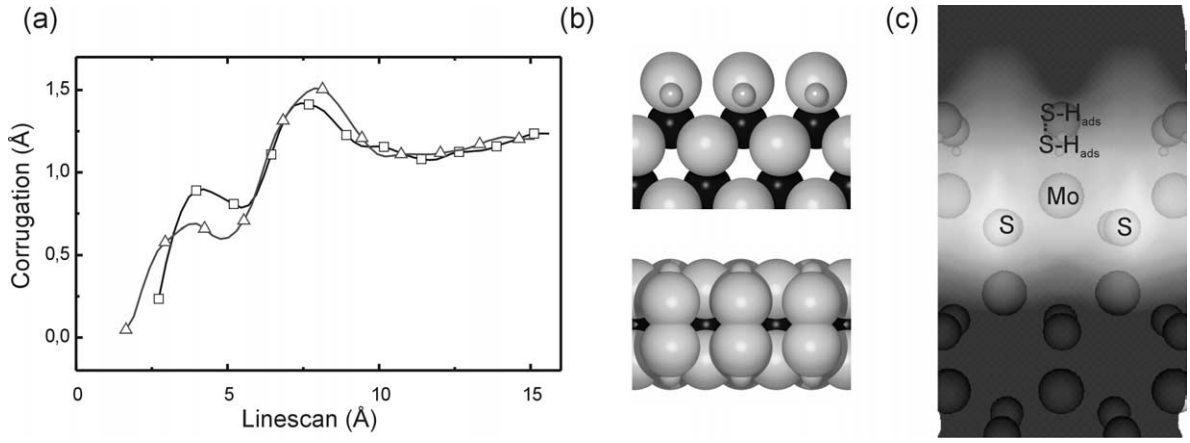

Fig. 5. (a) Representative STM line scans drawn perpendicularly to the fully sulfided Mo edge of the single-layer MoS_2 nanoclusters prior to (squares) and after (triangles) exposure to atomic hydrogen. The downshifted intensity of the outermost edge protrusions, corresponding to 0.2 Å, is associated with hydrogen atoms adsorbed on the edges. (b) Ball models of the proposed configuration in which hydrogen adsorbs on the fully sulfided Mo edges, shown in a top and side view representation. (c) STM simulation of the edge with hydrogen atoms adsorbed based on the Tersoff–Hamann theory. (Reprinted figure with permission from M.V. Bollinger, K.W. Jacobsen, J.K. Nørskov, Phys. Rev. B 67 (2003) 085410. Copyright 2003 by the American Physical Society.) The simulation is in quantitative and qualitative accordance with the experiment.

trusions primarily reflect the interstitial space between the S dimers with H adsorbed. Quantitatively, the adsorption of H, however, changes the local electronic structure near the S dimers and the simulated STM image reproduces the downshift of the edge protrusions in agreement with the STM findings, although a slightly smaller value of ~ 0.1 Å is found.

According to DFT calculations the H atoms adsorbed on the S dimers (Fig. 5b) are in fact marginally unstable (energy of $+0.17$ eV) relative to molecular H_2 [26]. Hydrogen adsorbed in other geometries on the fully sulfided Mo edges has recently been found to be slightly more stable [43], but these geometries are, however, not directly relevant to the present STM experiments, since they most probably would introduce structural features along the edges of the MoS_2 nanocluster which are not apparent in the atom-resolved STM images. It is suggested that an energy barrier exists, which under the conditions of our experiment prevents the desorption of hydrogen from the adsorption configuration in Fig. 5b [44], and since this implies a similar barrier for the dissociative adsorption of H_2, it also explains the need experimentally to predissociate H_2. At present no direct observations are available, but it is a possibility that an energetically favorable dissociation pathway for the formation of S–H groups exists through interaction of hydrogen molecules with the metallic brim sites on the Mo edge. We have undertaken studies to shed more light on this dissociation pathway. Under real reaction conditions, however, the high temperatures and high partial pressure of hydrogen gas are expected to allow for hydrogen dissociation to occur rapidly, and that the edges will maintain a reasonable coverage of S–H groups. The use of atomic hydrogen in this experiments can therefore be viewed as a simple way of providing hydrogen atoms at the high chemical potential found under real reaction conditions.

On this basis and the fact that hydrogen is necessary for a strong interaction in the experiments, the molecular species observed in Fig. 4 are suggested to be the result of thiophene molecules which have undergone a hydrogenation reaction on the brim sites near the edges. Presumably, the combination of having hydrogen atoms adsorbed at the edges in the form of S–H groups and the unusual sites for thiophene adsorption on the metallic brim in Fig. 4 presents a favorable situation for a hydrogenation reaction. In view of this, molecules, in which either one or both of the double bonds of thiophene have become hydrogenated, seem to be the most likely candidates as adsorbed intermediate species, but as will be evident below, the special electronic environment at the metallic edges can also facilitate a destabilization of the C–S bond, and therefore other ring-opened molecules have been considered as well.

3.5. Reaction pathway and energetics

In order to elucidate the identity of the species observed in the STM experiments, we have extended the previous DFT calculations [15] and considered a number of different thiophene-derived molecules adsorbed in a repeated geometry along the Mo edge of MoS_2. In accordance with the low-temperature STM experiments and earlier estimates of thiophene desorption temperatures on supported MoS_2 catalyst particles [40], the first DFT results show that pure thiophene indeed interacts only very weakly with the fully sulfided edges of MoS_2. The first two steps in the energy diagram in Fig. 8b demonstrate that adsorption of thiophene from the gas phase on the metallic brim is associated with an energy gain of only 0.2 eV per molecule, which corresponds closely to the rather low desorption temperature found in the experiments discussed above (Section 3.2).

We have then investigated adsorption configurations of 2,3-dihydrothiophene (C_4H_6S), 2,5-dihydrothiophene

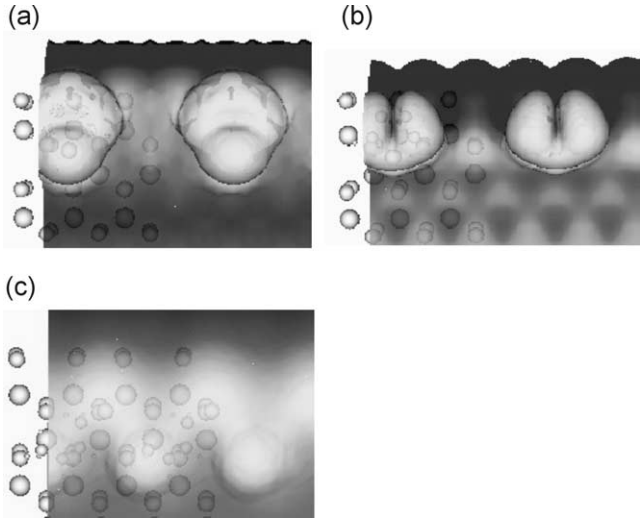

Fig. 6. Selected examples of STM simulations of different molecules adsorbed in a repeated geometry on the Mo edge of MoS_2. The images show (a) Thiophene (C_4H_4S), (b) 2,5-dihydrothiophene, and (c) *cis*-but-2-ene-thiolate (C_4H_7S), respectively. Atomic balls imbedded in the STM simulation indicate the position of Mo (large) and S (small) atoms of the MoS_2 nanocluster edge.

(C_4H_6S), tetrahydrothiophene (C_4H_8S), butenethiolates (C_4H_7S), and butanethiolate (C_4H_9S) on the fully sulfided Mo edge of MoS_2 by density-functional theory calculations and simulated their appearance in STM images. The STM simulations illustrated in Fig. 6 show three examples of thiophene, 2,5-dihydrothiophene, and *cis*-but-2-ene-thiolate, respectively. From these, the STM simulation of the ring-opened C_4H_7S compound in Fig. 6c is in particular seen to show good accordance with the experimental STM results, whereas the others show little resemblance. The characteristics associated with each C_4H_7S molecule in the simulation are shown in greater detail in Fig. 7b, and it indeed reproduces most of the important features found in the STM image in Fig. 7a, including the shifted intensity of the three outermost protrusions near the molecular adsorption site and the bean-like structure behind the brim, which is seen to be associated with the ring-opened carbon chain of the thiolate, the end group of which is imaged with a higher intensity. We therefore conclude that the reaction intermediates observed in the STM image in Fig. 4 are *cis*-but-2-ene-thiolates.

To further resolve the nature of the reaction intermediates found in the STM experiments, the DFT calculations were used to elucidate the possible reaction pathways and energetics involved. The reaction scheme and the corresponding energy diagram in Figs. 8a and b illustrate the proposed reaction pathway leading to the adsorbed C_4H_7S state. Starting from the physisorbed thiophene molecules with adsorption energies (ΔE_{ads}) of less than 0.2 eV per molecule, one of the double bonds in thiophene is hydrogenated causing the other double bond to shift; i.e., 2,5-dihydrothiophene adsorbed to the cluster edge is formed. In the next step, a calculation of the activation barrier is included in Fig. 8b for what is assumed to be the most difficult step in the reaction, the C_α–S bond cleavage. It is interesting to note that the associated barrier is rather modest ($E_a = 1.07$ eV). At the temperature (500 K) where thiophene reacts on the MoS_2 nanoclusters, this means that the equilibrium between C_4H_7S and thiophene in the gas phase is easily achieved. The same is of course true under industrial hydrotreating conditions. If we assume a simple Arrhenius behavior, a barrier of $E_a = 1.07$ eV implies a turn-over-frequency of approximately $10^{13} \cdot \exp(-E_a/k_BT) \approx 10^5$ reactions per second at 673 K; i.e., the reaction into thiolates may proceed with a significant rate under typical catalytic operating conditions. The barrier for the reverse reaction is, however, large enough for thiophene not to be desorbed during STM imaging at room temperature, which explains the experimental observations.

The final configuration (iii) in Fig. 8b associated with the ring-opened thiolate structure on the cluster edge corresponds to a simple adsorbed thiol. The observation of these thiolate intermediates is interesting, since thiols are much more reactive that thiophenes under real HDS conditions [6]. This is, however, fully explained by the conditions of the STM experiment and the barrier of desorption for the thiolates. After the first C–S bond in thiophene has been broken, the sulfur is much more reactive. The final C–S bond breakage is, however, likely to require a site capable of accepting sulfur and may thus take place at another site on the cluster. Such sites are presumably sulfur vacancies located at the edge [6,12,30], and surface diffusion of the thiolates along the edge or through the gas phase (after recombination with adsorbed H) to vacancies is therefore needed for the final step in the overall reaction process. From the consecutive series of STM images illustrated in Fig. 9, a mobility of the adsorbed thiolate species is indeed observed, supporting that the reactivity can be explained by a two-step process in which the thiophene is first hydrogenated, the first C–S bond is cleaved on the brim sites and subsequently the ring-opened molecule is transported to a sulfur vacancy on the cluster edge where the second C–S bond can be broken. The final S extrusion on a vacancy was not observed directly in these dynamic STM studies, since the present experiments, performed under UHV at room temperature, capture the model catalyst in a fully sulfur-saturated situation, disabling the continued reaction of thiolates. Unlike during real continuous HDS conditions, the number of available S vacancies is depleted once the atomic-hydrogen flux is terminated due to the recombination with S from dosed molecules prior to imaging. By quickly cooling the sample in the STM to temperatures below 240 K after the thiophene flux was terminated, it was, however, possible in a very few instances to capture species attached to the edge in a configuration that indicated a direct end-on bonding. This is illustrated in Fig. 10. In view of the spherical appearance of the adsorbate on the cluster edge, we tentatively associate the species with η_1-coordinated thiophene rather than a thiolate.

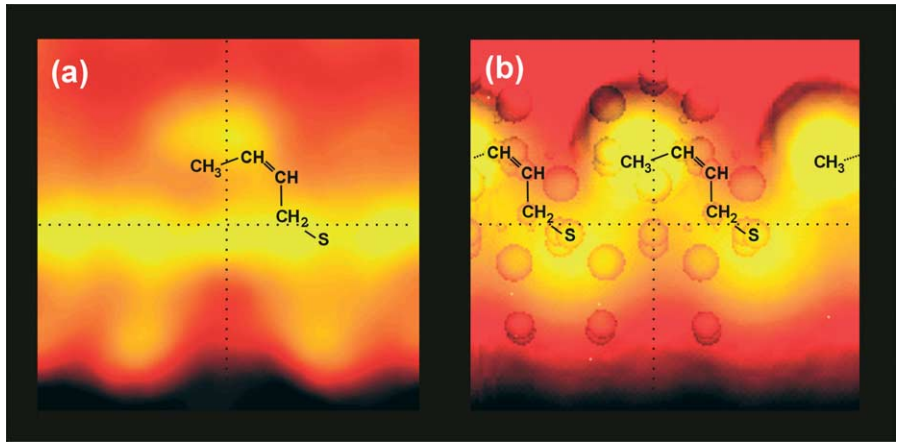

Fig. 7. (a) Close-up of an STM image showing a single *cis*-but-2-ene-thiolate (C_4H_7S) molecule adsorbed on the metallic brim. (b) STM simulation of the same part of the MoS_2 nanocluster. Atomic balls imbedded in the STM simulation indicate the position of Mo (large) and S (small) atoms of the MoS_2 nanocluster edge. The molecular skeleton model shows the thiolate structure and its most stable configuration found from the DFT calculations.

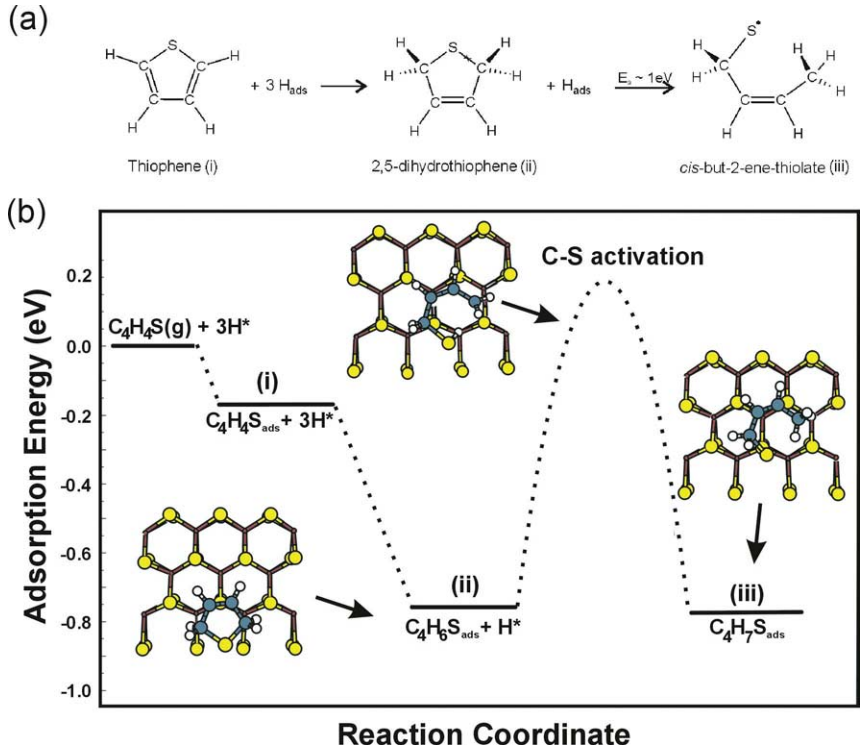

Fig. 8. (a) The proposed reaction scheme of thiophene leading to the thiolate intermediates observed with STM. All processes occur while the reactants are adsorbed on the fully sulfided Mo edge of the MoS_2 nanoclusters. For clarity, only thiophene and H reactants are shown. (b) The calculated energies associated with the individual steps in the reaction path (above) of thiophene species adsorbed on sites on the metallic edge state of MoS_2. The energies are in eV and are calculated relative to gas-phase thiophene and H adsorbed on the fully sulfided Mo edge ($\Delta E_H \approx +0.17$ eV). The diagram displays the most relevant intermediate steps in the hydrogenation of thiophene and subsequent C_α–S bond cleavage. Labels refer to the schematic representation above. The ball-and-stick models illustrate the geometric configurations associated with adsorbed species before, during and after C_α–S bond cleavage. The final configuration is C_4H_7S (*cis*-but-2-ene-thiolate). The position and geometry of the molecule adsorbed on the cluster are also illustrated in Fig. 5. Note the modest activation barrier associated with the last step, (ii) to (iii), $E_a = 1.07$ eV.

4. Discussion

The STM results demonstrate the first direct atomic-scale information of thiophene HDS reaction pathways on MoS_2 nanoclusters and the findings have several important implications in terms of explaining the reactivity of MoS_2 nanoclusters. It is observed that thiophene HDS may proceed by a mechanism very different from that advocated in earlier proposals [45–49]. In particular, by identifying reaction intermediates a new route is identified for activating a sulfur-containing molecule like thiophene, which takes place by hydrogenation of the double bonds followed by a C–S

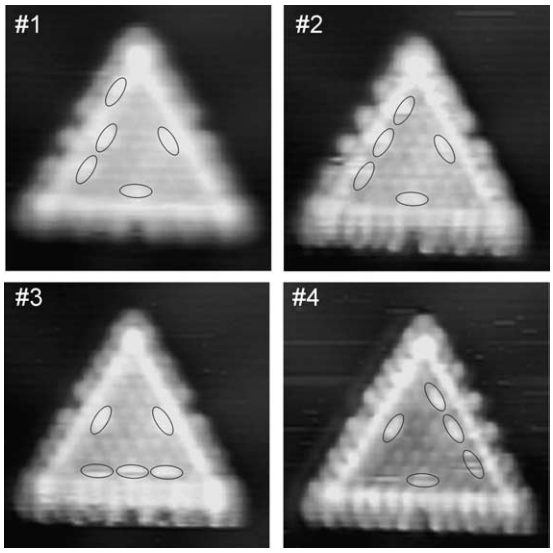

Fig. 9. Sequence of STM images of the same MoS_2 triangle showing several adsorbed C_4H_7S species (each indicated with a black ellipse). The time lapse between images is on the order of 1 min. In this time interval, individual species have moved to other sites on the cluster, indicating a considerable mobility of the adsorbed species along the one-dimensional metallic edge state.

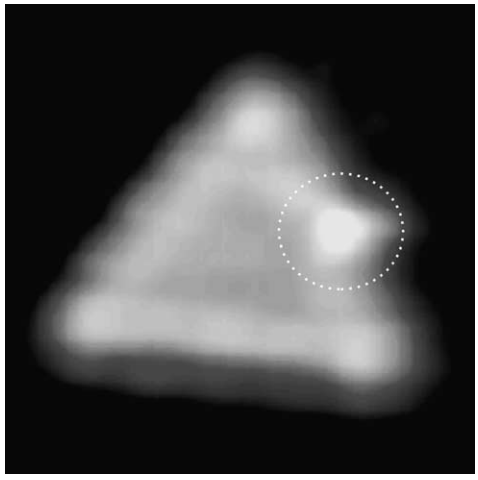

Fig. 10. STM image of a triangular MoS_2 nanocluster exposed first to atomic hydrogen, then thiophene, and finally quenched to an imaging temperature of 250 K in the cold STM. The large protrusion near the edge (indicated by a circle) possibly identifies with either an intact thiophene molecule coordinated end-on to a vacancy or a hydrogenated derivative coordinated through the terminal S atom.

bond breaking. Remarkably, the brim sites adjacent to the completely sulfur-saturated Mo edge are able to not only catalyze the hydrogenation of the carbon double bonds in the presence of neighboring S–H groups but also to activate and break up the first C–S bond of the hydrogenated thiophene. All the processes take place on top of specific sulfur atoms of the MoS_2 nanoclusters with no direct interaction with the Mo atoms. The interesting chemistry is clearly associated with the metallic character of the brim sites located adjacent to the MoS_2 edges. No indication of chemical activity is found experimentally or theoretically at the interior S atoms on the MoS_2 basal plane. The metallic states associated with the brim sites, on the other hand, have the ability to donate and accept electrons and thus act as catalytic sites very much like ordinary catalytically active metal surfaces. Whereas many catalytically active metal surfaces (Fe, Ni, Mo to mention a few [50–54]) are poisoned by H_2S and strongly bonded sulfur residues, the fully sulfur-coordinated brim sites of the MoS_2 nanoclusters are clearly not. Compared to the reactive metals on one hand and the inert basal plane of the MoS_2 nanoclusters on the other, the metallic brim sites seem to offer a more optimum bonding strength for the adsorption of thiophene. This kind of interaction is a compromise with an intermediate adsorption strength of the reactant which generally characterizes a good catalyst [55,56].

The existence of brim sites and their role in hydrogenation reactions as inferred directly from the present atomic-scale studies explain the results of many other studies treating the kinetics and mechanisms of HDS catalysis. Furthermore, the present results are consistent with many previous structure–activity correlations (see e.g., [6]), which have concluded that the activity is related to the MoS_2 edges. This is linked to the fact that the number of brim sites is roughly proportional to the number of edge sites. Valuable information on the selectivity of the catalyst has been obtained in other studies by selectively poisoning the active sites in the catalyst with different molecules while simultaneously monitoring the reaction rates. In such inhibition studies, H_2S is in general found to severely inhibit the HDS reaction of thiophene and other S-containing compounds, most likely due to vacancy recombination, whereas the HYD reaction of aromatic-like compounds is found to be only slightly influenced [6,48,57]. This simple observation can readily be explained by considering the metallic brim sites, since atom-resolved in situ STM imaging of the triangular MoS_2 nanoclusters in a 10^{-6} mbar H_2S atmosphere did not reveal any sign of H_2S adsorption on the brim sites; i.e., H_2S does not compete with the suggested HYD active sites, whereas a strong affinity to vacancies exists [30,31]. On the other hand, the HYD activity of the real catalyst is generally observed to be severely inhibited during simultaneous reaction with more electronegative, N-containing, aromatic compounds like pyridine (C_5H_5N) or quinoline (C_9H_7N) [57–59], implying that these molecules adsorb initially on similar sites as thiophene on the brim sites of the MoS_2 nanoclusters. Since the hydrogenation of such nitrogen-containing aromatics is also an integral part of the hydrodenitrogenation (HDN) process by MoS_2-based catalysts [6,60–62], we therefore suggest that the chemical activity associated with sites on the metallic edge states of MoS_2 may be of general importance for hydrogenation reactions of the wealth of other unsaturated molecules present in crude oil. In future experiments it will be interesting to test this by exposing the clusters to N-containing molecules and to

investigate the exact interaction of these with the MoS_2 nanoclusters with STM.

Based on our findings, we propose an HDS mechanism in which both the brim sites and neighboring S–H groups are involved in the first hydrogenation (HYD) reaction and subsequent C–S cleavage of one of the bonds in thiophene. This reaction in presumably followed by S extrusion from the formed thiolate intermediate on a sulfur vacancy. The brim sites associated with metallic edge states of the MoS_2 nanoclusters are responsible for binding thiophene to the clusters, and the hydrogenation reaction is driven by the nearby S–H groups which provide a source of highly reactive H atoms. In this way, an alternative *two-step* reaction path is offered by the clusters in parallel with the direct extrusion path of S from thiophene on vacancies. This "traditional" way of considering the HDS reaction of thiophene by direct coordination of the S to one or more undercoordinated Mo atoms is thus not excluded from the present studies. In fact, the spherically shaped features observed at low temperature in Fig. 10 may represent an η_1 binding of thiophene to a vacancy. Both the direct extrusion pathway of S in thiophene and the more elaborate mechanism involving the brim sites suggested here from the STM findings are therefore likely to prevail for thiophene under operating conditions.

A discussion of whether the proposed two-step HDS reaction process of thiophene is also relevant for reactions of other and more complicated molecules present in the oil feed. Thiophene was chosen for this study as it represents a standard test molecule, but it does in fact not represent the major obstacle in achieving deep HDS. Dibenzothiophenes and especially the substituted derivatives, e.g., 4,6-dimethyldibenzothiophene, present a much bigger problem due to sterical hindrance [2,6,63,64]. For such molecules, the reaction pathway proceeding by prehydrogenation and bond cleavage is more important than direct S extrusion. This fact has been attributed to steric hindrance of the end-on coordination of S in the larger molecules. The lower steric sensitivity toward the prehydrogenation pathway has, however, remained controversial. In one study, Ma and Schobert [65] suggested that hydrogenation could occur on multiple vacancy sites, and other studies have suggested that such sites could be formed, for example, on the Mo edge. Density-functional calculations have, however, shown that such sites are energetically very unfavorable and one would expect an extreme sensitivity toward poisoning by H_2S. The present suggestion that the hydrogenation path involves the brim sites allows these observations to be reconsidered. Indeed, adsorption of the large molecules on the brim sites can be achieved through a good overlap with the π-electron system. This prehydrogenation route could then lead to bond cleavage in the more complicated structures and thus lower the sterically hindered access to the S heteroatom for the final S extrusion. In view of this proposal, the fact that the tendency to form π-bonds correlates with the hydrogenation rate of aromatics is highly interesting [66].

The results of a previous catalysts model study on structure–activity relationships also support the proposed model. In the "rim-edge" model proposed by Daage and Chianelli [67], unsupported catalysts were described as stacked MoS_2 crystallites. Based on steric considerations, the top (and bottom) layers of unsupported crystallites were suggested to have sterically hindered edge sites which are active in both the HYD and the HDS reactions, whereas the edges in the intermediate layers were suggested to be reactive in HDS reactivity only. The results have a clear interpretation in terms of the new mechanism presented presently. Preliminary STM results show that stacked MoS_2 nanoclusters also exhibit the bright brim associated with the metallic edge state [68], and evidently only the top layer of such stacked MoS_2 clusters will contain accessible brim sites and hence will be active in HYD. Vacancies, on the other hand, will most likely be created both on the top but also on lower lying layers in such stacked structures, thus exposing sites which are primarily active in direct HDS.

The concept of chemically active brim sites on MoS_2 nanoclusters may also be extended to the variety of other MoS_2-like structures that form under different conditions. We have recently presented the first atomic-scale images of the CoMoS structures present in Co-promoted, MoS_2-based HDS catalysts [13], and shown that the presence of the Co promoter atoms causes the shape of the MoS_2 nanoclusters to change from a triangular to a hexagonally truncated shape. We have also shown that hexagonally shaped MoS_2 nanoclusters may form under more hydrogen-rich conditions [14]. Both the CoMoS clusters and the MoS_2 hexagons formed under more reducing conditions are found to be terminated by different edge structures than those presented for the present MoS_2 triangles. Nevertheless, atom-resolved STM images show that they exhibit similar bright brims in the rows adjacent to the cluster edges. Although no direct experiments are available at this stage, some of the same processes involving reactions on metallic brim sites are proposed to occur also on these other types of MoS_2 or CoMoS edges. This could be an important part of Cobalt's promoting role, since the CoMoS nanoclusters with Co incorporated at the S edges display bright brims in the STM images with a very high intensity (> 1.0 Å) [13].

5. Conclusion

In conclusion, new detailed insight based on atom-resolved STM images suggests that two types of sites may be involved in the hydrotreating reactions on MoS_2 nanoclusters. Of special interest is the observation of a new kind of active sites associated with one-dimensional metallic brim sites of MoS_2 nanoclusters. These are quite unusual compared to the undercoordinated Mo edge atoms traditionally used to explain the reactivity of MoS_2 nanoclusters. The new insight is obtained by resolving both the electronic and the atomic-scale geometric structure of nanosized MoS_2 clusters

synthesized on a gold substrate as a suitable model system for the hydrotreating catalyst. Exactly this choice of model system allows us to probe the catalytically active sites on the atomic scale by carefully monitoring the response of the MoS_2 nanoclusters to hydrogen and thiophene (C_4H_4S) in atom-resolved STM images.

Acknowledgments

The authors gratefully acknowledge discussions with M. Bollinger and K.W. Jakobsen. This work was supported by the Danish National Research Foundation through the Center for Atomic-scale Materials Physics (CAMP). J.V.L. acknowledges support from the Danish Technical Research Council.

References

[1] I. Mochida, K. Sakanishi, X. Ma, S. Nagao, T. Isoda, Catal. Today 29 (1996) 185.
[2] D.D. Whitehurst, T. Isoda, I. Mochida, Adv. Catal. 42 (1998) 345.
[3] J.W. Gosselink, Cattech 4 (1998) 127.
[4] E. Derouane, Cattech 5 (2001) 214.
[5] H. Topsøe, K.G. Knudsen, L.S. Byskov, J.K. Nørskov, B.S. Clausen, Stud. Surf. Sci. Catal. 121 (1999) 13.
[6] H. Topsøe, B.S. Clausen, F.E. Massoth, in: Hydrotreating Catalysis, Science and Technology, vol. 11, Springer, Berlin, 1996.
[7] R. Prins, V.H.J. de Beer, G.A. Somorjai, Catal. Rev.-Sci. Eng. 31 (1989) 1.
[8] F.E. Massoth, G. Muraledhar, in: 4th Int. Conf. Climax, Ann Arbor, MI, 1983, p. 343.
[9] E. Payen, S. Kasztelan, J. Grimblot, J. Mol. Struct. 174 (1998) 71.
[10] P. Sundberg, R. Moyes, J. Tomkinson, Bull. Soc. Chim. Belg. 100 (1991) 967.
[11] N.-Y. Topsøe, H. Topsøe, J. Catal. 139 (1993) 641.
[12] S. Helveg, J.V. Lauritsen, E. Lægsgaard, I. Stensgaard, J.K. Nørskov, B.S. Clausen, H. Topsøe, F. Besenbacher, Phys. Rev. Lett. 84 (2000) 951.
[13] J.V. Lauritsen, S. Helveg, E. Lægsgaard, I. Stensgaard, B.S. Clausen, H. Topsøe, F. Besenbacher, J. Catal. 197 (2001) 1.
[14] J.V. Lauritsen, M.V. Bollinger, E. Lægsgaard, K.W. Jacobsen, J.K. Nørskov, B.S. Clausen, H. Topsøe, F. Besenbacher, J. Catal. 221 (2004) 510.
[15] J.V. Lauritsen, M. Nyberg, R.T. Vang, M.V. Bollinger, B.S. Clausen, H. Topsøe, K.W. Jacobsen, E. Lægsgaard, J.K. Nørskov, F. Besenbacher, Nanotechnology 14 (2003) 385.
[16] E. Lægsgaard, F. Besenbacher, K. Mortensen, I. Stensgaard, J. Microscopy 152 (1988) 663.
[17] F. Besenbacher, Rep. Prog. Phys. 59 (1996) 1737.
[18] F. Elfeniat, C. Fredriksson, E. Scaher, A. Selmani, J. Chem. Phys. 102 (1995) 6153.
[19] G. Liu, J. Rodriguez, J. Dvorak, J. Hrbek, T. Jirsak, Surf. Sci. 505 (2002) 295.
[20] G. Poirier, Chem. Rev. 97 (1997) 1117.
[21] F. Schreiber, Prog. Surf. Sci. 65 (2000) 151.
[22] A. Ulman, Self-Assembled Monolayers of Thiols, Thin Films, Academic Press, San Diego, CA, 1998.
[23] J. Perdew, J. Chevary, S. Vosko, K. Jackson, M. Pederson, D. Singh, C. Fiolhais, Phys. Rev. B 46 (1992) 6671.
[24] B. Hammer, J.K. Nørskov, Adv. Catal. 45 (2000) 71.
[25] Dacapo pseudopotential code. http://www.fysik.dtu.dk/campos.
[26] M.V. Bollinger, K.W. Jacobsen, J.K. Nørskov, Phys. Rev. B 67 (2003) 085410.
[27] H. Jonsson, G. Mills, K.W. Jacobsen, in: B.J. Berne, G. Ciccotti, D.F. Coker (Eds.), Classical and Quantum Dynamics in Condensed Phase Simulations, World Scientific, Singapore, 1998, pp. 385–404.
[28] J. Tersoff, D.R. Hamann, Phys. Rev. Lett. 50 (1983) 1998.
[29] M.V. Bollinger, J.V. Lauritsen, K.W. Jacobsen, J.K. Nørskov, S. Helveg, F. Besenbacher, Phys. Rev. Lett. 87 (2001) 196803.
[30] L.S. Byskov, J.K. Nørskov, B.S. Clausen, H. Topsøe, J. Catal. 187 (1999) 109.
[31] P. Raybaud, J. Hafner, G. Kresse, S. Kasztelan, H. Toulhoat, J. Catal. 189 (2000) 129.
[32] S. Cristol, J.F. Paul, E. Payen, D. Bougeard, S. Clémendot, F. Hutschka, J. Phys. Chem. B 104 (2000) 11220.
[33] J.F. Paul, E. Payen, J. Phys. Chem. B 107 (2003) 4057.
[34] H. Schweiger, P. Raybaud, G. Kresse, H. Toulhoat, J. Catal. 207 (2002) 76.
[35] K.K. Kam, B.A. Parkinson, J. Phys. Chem. 86 (1982) 463.
[36] T. Böker, R. Severin, A. Müller, C. Janowitz, R. Manzke, D. Voss, P. Krüger, A. Mazur, J. Pollmann, Phys. Rev. B 64 (2001) 235305.
[37] M. Salmeron, G. Somorjai, A. Wold, R. Chianelli, K. Liang, Chem. Phys. Lett. 90 (1982) 105.
[38] P.C.H. Mitchell, D.A. Green, E. Payen, J. Tomkinson, S.F. Parker, Phys. Chem. Chem. Phys. 1 (1999) 3357.
[39] P. Mills, S. Korlann, M.E. Bussell, M.A. Reynolds, M.V. Ovchinnikov, R.J. Angelici, C. Stinner, T. Weber, R. Prins, J. Phys. Chem. A 105 (2001) 4418.
[40] T.L. Tarbuck, K.R. McCrea, J.W. Logan, J.L. Heiser, M.E. Bussell, J. Phys. Chem. B 102 (1998) 7845.
[41] K.-F. Braun, K.-H. Rieder, Phys. Rev. Lett. 88 (2002) 096801.
[42] W. Di, K.E. Smith, S.D. Kevan, Phys. Rev. B 45 (1992) 3652.
[43] S. Cristol, J.F. Paul, E. Payen, D. Bougeard, S. Clémendot, F. Hutschka, J. Phys. Chem. B 106 (2002) 5659.
[44] L.S. Byskov, M. Bollinger, J.K. Nørskov, B.S. Clausen, H. Topsøe, J. Mol. Catal. A: Chem. 163 (2000) 117.
[45] J.M.J. Lipsch, G.C.A. Schuit, J. Catal. 15 (1969) 174.
[46] S. Kolboe, Can. J. Chem. 47 (1969) 352.
[47] H. Kwart, G.C.A. Schuit, B.C. Gates, J. Catal. 61 (1980) 128.
[48] R. Ramachandran, F.E. Massoth, Can. J. Chem. Eng. 60 (1982) 17.
[49] N.N. Sauer, E.J. Markel, G.L. Schrader, R.J. Angelici, J. Catal. 117 (1989) 295.
[50] S.L. Bernaseka, L. Chenga, A.B. Bocarslya, T.A. Ramanarayananb, Surf. Sci. 374 (1997) 357.
[51] J. Stöhr, E.B. Kollin, D.A. Fischer, J.B. Hastings, F. Zaera, F. Sette, Phys. Rev. Lett. 55 (1985) 1468.
[52] J.A. Rodriguez, J. Dvorak, T. Jirsak, Surf. Sci. 457 (2000) L413.
[53] A. Gellman, M.H. Farias, M. Salmeron, G.A. Somorjai, Surf. Sci. 136 (1984) 217.
[54] R.I.R. Blyth, F. Mittendorfer, J. Hafner, S.A. Sardar, R. Duschek, F.P. Netzer, M.G. Ramsey, J. Chem. Phys. 114 (2001) 935.
[55] R. Chianelli, G. Berhault, P. Raybaud, S. Kasztelan, J. Hafner, H. Toulhoat, Appl. Catal. A 227 (2002) 83.
[56] J.K. Nørskov, T. Bligaard, A. Logadottir, S. Bahn, L.B. Hansen, M. Bollinger, H. Bengaard, B. Hammer, Z. Sljivancanin, M. Mavrikakis, Y. Xu, S. Dahl, C.J.H. Jacobsen, J. Catal. 209 (2002) 275.
[57] M. Girgis, B.C. Gates, Ind. Eng. Chem. Res. 30 (1991) 2021.
[58] M. Nagai, T. Sato, A. Aiba, J. Catal. 97 (1986) 52.
[59] V. LaVopa, C. Satterfield, J. Catal. 110 (1988) 375.
[60] J.F. Cocchetto, C.N. Satterfield, Ind. Eng. Chem. Proc. Des. Dev. 20 (1981) 49.
[61] R. Prins, in: G. Ertl, H. Knözinger, J. Weitkamp (Eds.), Handbook of Heterogeneous Catalysis, VHC, Weinheim, 1997, p. 1908.
[62] R. Prins, Adv. Catal. 46 (2002) 399.
[63] N. Hermann, M. Brorson, H. Topsøe, Catal. Lett. 65 (2000) 169.
[64] B. Gates, H. Topsøe, Polyhedron 16 (1997) 3213.
[65] X.L. Ma, H.H. Schobert, ACS Div. Petrol Chem. Prepr. 213 (1997) 15.
[66] N.K. Nag, Appl. Catal. 10 (1984) 53.
[67] M. Daage, R.R. Chianelli, J. Catal. 149 (1994) 414.
[68] J.V. Lauritsen, PhD thesis, University of Aarhus, 2002.